

MOL 39321

An Intracellular, Allosteric Site for a Specific Class of Antagonists of the CC Chemokine G Protein-Coupled Receptors, CCR4 and CCR5

Glen Andrews, Carolyn Jones and Keith A. Wreggett[†]

Departments of Discovery BioScience (GA and KAW) and Molecular Biology (CJ), Respiratory and Inflammation Research Area, AstraZeneca Research and Development, Loughborough, U.K.

MOL 39321

Running title: Intracellular allosteric site for chemokine GPCR antagonists

Address correspondence to:

Dr Keith Wreggett

Department of Discovery BioScience

AstraZeneca R&D Charnwood

Bakewell Road

Loughborough, Leicestershire, LE11 5RH, U.K.

Tel: +44 1509 644000, Fax: +44 1509 645506

email: keith.wreggett@astrazeneca.com

Manuscript information:

Number of text pages: 48

Number of tables: 2

Number of figures: 11

Number of references: 40

Number of words in the abstract: 237

Number of words in the introduction: 730

Number of words in the discussion: 1500

ABBREVIATIONS: [³H]Cmpd-1, 5-Chloro-*N*-(5,6-dichloro-3-[1,1,1-³H]methoxy-pyrazin-2-yl)thiophene-2-sulfonamide; BMS-397, *N*-(2,4-dichlorobenzyl)-2-{4-[(2*R*)-piperidin-2-ylcarbonyl]piperazin-1-yl}pyrido[2,3-*d*]pyrimidin-4-amine; BSA, bovine serum albumin; CCR3, CC chemokine receptor 3; CCR4, CC chemokine receptor 4; CCR4-5T, CCR4 with the C-terminal domain of CCR5; CCR5, CC chemokine receptor 5; CCR5-4T,

MOL 39321

CCR5 with the C-terminal domain of CCR4; CHO, Chinese Hamster Ovary cell line; CXCR2, CXC chemokine receptor 2; DMSO, dimethyl sulfoxide; FB, FMAT-Blue fluorescent dye; FLIPR, fluorometric imaging plate reader; FMAT, fluorometric microvolume assay technology; GPCR, G protein-coupled receptor; Gq_{i5}, Gq protein alpha subunit with the last 5 C-terminal amino acids replaced with those from Gi protein alpha subunit; HEK, human embryonic kidney cell line HEK293; PBS, phosphate-buffered saline; pEC₅₀, the molar concentration of an agonist that achieves 50% of the maximal response; pIC₅₀, the negative logarithm to base 10 of the molar concentration of an antagonist that reduces the control response by 50%; pK_d, the negative logarithm to base 10 of the equilibrium dissociation constant; SCH-C (SCH 351125), (4-bromophenyl) {1'-[(2,4-dimethyl-1-oxido-pyridin-3-yl) carbonyl]-4'-methyl-1,4'-bipiperidin-4-yl} methanone O-ethyloxime.

MOL 39321

ABSTRACT

A novel mechanism for antagonism of the human chemokine receptors CCR4 and CCR5 has been discovered with a series of small-molecule compounds that appears to interact with an allosteric, intracellular site on the receptor. The existence of this site is supported by a series of observations: 1) intracellular access of these antagonists is required for their activity, 2) specific, saturable binding of a radiolabeled antagonist requires the presence of CCR4 and 3) through engineering receptor chimeras by reciprocal transfer of C-terminal domains between CCR4 and CCR5, compound binding and the selective structure-activity relationship for antagonism of these receptors appears to be associated with the integrity of that intracellular region. Published antagonists from other chemical series do not appear to bind to the novel site, and their interaction with either CCR4 or CCR5 is not affected by alteration of the C-terminal domain. The precise location of the proposed binding site remains to be determined, but the known close association of the C-terminal domain, including Helix 8, as a proposed intracellular region that interacts with transduction proteins (e.g., G Proteins and β -arrestin) suggests that this could be a generic allosteric site for chemokine receptors and perhaps more broadly for Class A G Protein-Coupled Receptors. The existence of such a site that can be targeted for drug discovery has implications for screening assays for receptor antagonists, which would need, therefore, to consider compound properties for access to this intracellular site.

MOL 39321

The super-family of G Protein-coupled receptors (GPCRs) represents a productive area for drug discovery. Worldwide sales of drugs that act via GPCRs were estimated in 2004 to be in excess of AM\$120 billion/year (Biopheonix, 2005). In that same year, chemical programs to target GPCRs accounted for 40% of the portfolio of the pharmaceutical industry, with nearly 40% of these in clinical development (Biopheonix, 2005).

Much of the progress in discovery of small molecule ligands (i.e., < 500 MW) for GPCRs comes from improvements in technologies to screen large numbers of compounds, where many campaigns will use functional assays with cell lines genetically engineered to express high amounts of the GPCR of interest, often co-expressed with a genetically modified G protein to improve signaling. This cell-based screening approach is supported by an understanding that the natural agonists for GPCRs interact with extracellular domains of the receptor that form a binding pocket, in analogy with the retinal-binding site of rhodopsin, and from mutagenesis studies of cloned GPCRs, which suggest that antagonists bind competitively at either the orthosteric or a syntopic site within the exofacial core of the transmembrane domains (Kristiansen, 2004). Structural modeling of GPCRs, based on homology with the resolved crystal structures of rhodopsin (Palczewski et al., 2000; Schertler, 2005), also is used to lead rational drug design and is centered on targeting the extracellular orthosteric site, (Kristiansen, 2004). Allosteric regulators of Class A GPCRs also exist, and although some of these are believed to make interactions with outer regions of the extracellular domain their actual sites of action are not yet known (Christopoulos, 2002; Birdsall and Lazareno, 2005).

MOL 39321

Receptors for chemoattract cytokines (chemokines) are Class A GPCRs that are believed to play a major role in diseases that include many inflammatory conditions, viral infections and cancers (Proudfoot, 2002; Saeki, 2004; Johnson et al., 2004). With peptide ligands almost 20-times the size of a small-molecule drug, the chemokine receptors were initially assumed to be an unlikely target for the identification of competitive antagonists. Following the discovery that small molecules can target chemokine receptors selectively, presumably through either syntopic competition or allosteric modulation, along with reports of their therapeutic potential in the clinic (e.g., Haringman et al., 2003), development of ligands at these GPCRs became a focus of activity in the pharmaceutical industry (Saeki, 2004; Johnson et al., 2004).

Identification of antagonists, such as SCH-C, at the CC chemokine receptor CCR5 has been the subject of considerable effort since it was identified as a co-receptor for the M-trophic form of HIV (Kazmierski et al., 2003). CCR5, having CCL3 (macrophage inflammatory protein 1 α ; MIP-1 α), CCL4 (macrophage inflammatory protein 1 β ; MIP-1 β) and CCL5 (regulated upon activation, normal T cell expressed and secreted chemokine; RANTES) as ligands, is also implicated in inflammatory diseases such as rheumatoid arthritis (Pralhad, 2006) and in autoimmune diseases such as multiple sclerosis and Type 1 diabetes (Proudfoot, 2002; Ajuebor et al., 2006).

As the receptor for the CC chemokine ligands CCL17 (thymus and activation-regulated chemokine, TARC) and CCL22 (macrophage-derived chemokine, MDC), CCR4 has been identified as a potentially important drug target for the treatment of T cell-mediated inflammatory diseases such as asthma and atopic dermatitis (Panina-Bordignon et al., 2001; Schuh et al., 2002; Homey et al., 2006). CCR4 is also suggested to have a role

MOL 39321

in cancer, including some T cell lymphomas and immunomodulation of tumor immunity through regulatory T cells Ferenczi et al., 2002; Ishida and Ueda, 2006). Progress in the discovery of small molecule CCR4 antagonists, such as BMS-397, has been reviewed recently (Purandare and Somerville, 2006).

A novel series of CCR4 antagonists was discovered by using a high-throughput recombinant cell-based functional assay of the activity of the CCR4 agonist, CCL22 (Baxter et al., 2003a; 2003b; 2005). The general properties of this pyrazinyl-sulfonamide series, including their high degree of selectivity against a wide range of receptors and other molecular targets, will be described elsewhere. Further work demonstrated that these compounds, whilst highly selective for CCR4, were also much weaker antagonists with a very similar structure-activity relationship at CCR5. In the course of a program to develop these antagonists an emerging pattern became clear for some compounds, having properties that deviated from the typical correlation of activity when comparing assays with membranes to those with intact cells. A study of these apparent outliers suggested that this entire series of CCR4 and CCR5 antagonists acts through a novel allosteric mechanism.

MOL 39321

Materials and Methods

Materials. HEPES, sodium chloride, magnesium chloride, sodium hydroxide and DMSO were from Sigma-Aldrich (Poole, UK). Bovine serum albumin (BSA) was obtained from Fluka (Gillingham, UK). Polypropylene 96-well plates and vented-cap cell culture flasks were from Costar (Corning, UK). Poly-D-lysine-coated 96-well plates were obtained from Becton Dickinson (Oxford, UK). Heat-inactivated fetal calf serum was from Sigma-Aldrich (Poole, UK). All other tissue culture reagents were purchased from Life Technologies (Paisley, UK). MicroScint-O was from Perkin Elmer (Boston, USA). Fluo-3 AM was from Molecular Probes (Paisley, UK). FuGENE 6 was obtained from Roche Diagnostics (Lewes, UK). Recombinant human, BSA-free chemokines were from R&D Systems (Abingdon, UK). FMAT-Blue-labeled (FB-) CCL5 and CCL22 were purchased from Applera (Warrington, UK). Reagents for the polymerase chain reaction (PCR) were supplied by Abgene (Epsom, UK). All other chemical reagents were analytical grade from Fisher Scientific (Loughborough, UK).

All of the chemokine antagonists described in this paper (see chemical structures in Figure 1) were supplied by the Department of Medicinal Chemistry, AstraZeneca Research and Development. Antagonists of the pyrazinyl-sulfonamide series were synthesized by using procedures similar to those disclosed (Baxter et al., 2003a; 2003b; 2005). [³H]Cmpd-1 [5-Chloro-*N*-(5,6-dichloro-3-[1,1,1-³H]methoxy-pyrazin-2-yl)thiophene-2-sulfonamide] was prepared (2830.5 GBq/mmol) by displacement of the 3-chloro-substituent of the 3,5,6-trichloropyrazine derivative using tritiated methanol. SCH-C and BMS-397 were synthesized by using methods similar to those disclosed (Palani et al., 2001; Purandare, 2004).

MOL 39321

Culture and source of stable recombinant cell lines. Cells were cultured in a humidified atmosphere of 5% (v/v) CO₂ in air at 37 °C in a standard incubator. CHO cells stably expressing human recombinant CCR4 (CCR4-CHO), obtained from Euroscreen (Brussels, Belgium), were cultured in NUT.MIX.F_12(HAM) medium with Glutamax-1 containing 10% (v/v) fetal calf serum and 0.4 mg/ml geneticin. CHO cells stably expressing human recombinant CCR5 (CCR5-CHO), prepared by ligation of CCR5 cDNA isolated from human peripheral blood lymphocytes into pcDNA3.1 (Invitrogen), were cultured in DMEM medium containing 10% (v/v) fetal calf serum and 1 mg/ml geneticin. HEK cells expressing human recombinant CCR4 (CCR4-HEK), prepared by ligation of CCR4 cDNA isolated from human Th2 lymphocytes into pIRESneo2 (Clontech), were cultured in DMEM medium with 2 mM glutamine and non-essential amino acids, containing 10% (v/v) fetal calf serum and 0.5 mg/ml geneticin. An HEK line stably transfected with a plasmid expressing a human chimeric G alpha subunit, Gq_{i5} (Gq alpha with the last 5 C-terminal amino acids replaced with those from Gi alpha), was obtained from Molecular Devices (Wokingham, UK). HEK-Gq_{i5} cells were cultured in DMEM medium with 2 mM glutamine and non-essential amino acids, containing 10% (v/v) fetal calf serum and 0.3 mg/ml hygromycin B. HEK-Gq_{i5} cells expressing human recombinant chemokine receptors were cultured in similar media but with the addition of 0.5 mg/ml geneticin.

Generation of plasmids for transient transfection. Chimeric CCR4 and CCR5 were assembled from DNA fragments that were generated by splice overlap extension PCR (Horton et al., 1989). The cDNA sequences of the clones that were used as templates for PCR fragment generation were the same as GenBank accession numbers AB02388

MOL 39321

(CCR4 - apart from 4 silent base substitutions: T24C, T279C, C1044T and C1098T; numbering starts from the beginning of the coding sequence) and AF031237 (CCR5). Predicted protein sequences of CCR4 and CCR5 were aligned, and a region of high homology within TM7 (shown below as boxed in Fig. 2) was chosen as the region of overlap used to generate the chimeras. 5'- and 3'-primers for PCR were designed to include restriction sites compatible with the expression vector (NheI and NotI; Roche). Joined PCR fragments corresponding to bases 1-911 of CCR4 fused to bases 890-1059 of CCR5 and bases 1-864 of CCR5 fused to bases 885-1083 of CCR4 were cloned into the mammalian expression vector pcDNA3.1 (Invitrogen), to provide resultant protein products corresponding to CCR4 amino acids 1-304 fused to CCR5 amino acids 298-352 (designated CCR4-5T) and CCR5 amino acids 1-288 fused to CCR4 amino acids 296-360 (designated CCR5-4T). Vectors for full-length wild type CCR4 and CCR5 were similarly prepared.

Generation of transient recombinant cells. Transient expression in HEK-Gq_{i5} cells was made by using FuGENE 6 with relevant plasmids, and was performed in 225 cm² flasks according to the supplier's instructions. Briefly stated, a suspension of 13 X 10⁶ cells in culture medium without antibiotics was added to flasks and cells were allowed to adhere overnight before addition of 16 µg of plasmid cDNA that was pre-mixed with Optimem containing FuGENE 6. The cells were incubated with cDNA for 24 h prior to seeding into 96-well plates and then a further 24 h prior to use in calcium-signaling or antagonist binding assays.

Binding of FB-CCL22 and -CCL5 to recombinant cells. Binding of FMAT-Blue labeled (FB-) chemokines was performed essentially as described by Mellentin-

MOL 39321

Michelotti et al., 1999. Recombinant CHO cells were seeded in culture medium at 1×10^4 /well in black, clear-bottomed, 96-well plates and then incubated overnight. Cells were washed with Assay Buffer (20 mM HEPES, Hanks Balanced Salt Solution, pH 7.4 at 20 °C with NaOH) before adding a compound, agonist or appropriate vehicle. Binding was initiated by addition of FB-CCL5 or -CCL22 (1 nM final concentration) in Assay Buffer. After incubation for 3 h at room temperature, the median, cell-associated fluorescence in each well was measured by using an Applied Biosystems 8200 Cellular Detection System.

Cell membrane preparation. Wild-type or recombinant CHO cells were removed from cell culture flasks with 2 mM EDTA in PBS and then harvested by centrifugation at 350 g for 5 min at room temperature. The cell pellet was re-suspended at a density of 1×10^7 cells per ml in ice-cold buffer (20 mM HEPES, 1 mM EDTA, 3 mM benzamidine, 1 mM PMSF, 100 µg/ml bacitracin, 1 µg/ml leupeptin and 2 µg/ml soybean trypsin inhibitor, pH 7.4 at 22 °C with NaOH). The cell suspension was homogenized (2 X 30 s) by using a Polytron hand-held homogenizer, and then centrifuged at 1000 g for 15 min. The resultant supernatant was centrifuged at 100000 g for 30 min at 4 °C. The resultant membrane pellet was re-suspended at 1×10^8 cell equivalents per ml in the homogenization buffer containing 1% (v/v) glycerol, and then stored at -80 °C.

Antagonist binding to intact recombinant cells or membranes. Binding Buffer (20 mM HEPES, 50 mM NaCl, 5 mM MgCl₂, pH 7.4 at 22 °C with NaOH) containing either a test compound or appropriate vehicle was added to [³H]Cmpd-1 (1 nM final concentration) in a 96-well polypropylene plate, and binding initiated by addition of either membranes (typically 15 µg per well) or intact cells (typically 2×10^4 CHO cells per

MOL 39321

well or 8×10^4 HEK cells per well) in Binding Buffer. After incubation to steady-state for 1 h at room temperature, the content of each well was passed through a Packard Unifilter GF/B plate, which was then washed with 4 X 350 μ l Binding Buffer at 4 °C and then dried for at least 1 h at 50 °C. Filter-bound radioactivity was measured (45% efficiency; TOPCOUNT, Packard BioScience) after addition of 50 μ l of MicroScint-O to each well.

Calcium-signaling in recombinant cells. Recombinant cells were seeded in culture medium at 5×10^4 /well in black, clear-bottomed, poly-D-lysine-coated, 96-well plates and then incubated overnight. Cells loaded with Fluo-3AM in FLIPR Buffer [20 mM HEPES, 0.15 M NaCl, 5 mM KCl, 1 mM CaCl_2 , 1 mM MgCl_2 , 5 mM D-glucose, 0.01% (w/v) BSA, pH 7.4 at 22 °C with NaOH] were briefly washed with FLIPR Buffer at 37 °C. Test compounds (or vehicle controls) in FLIPR Buffer were then pre-incubated with the cells for 15 min before transfer of the plate to either a FLIPR or a TETRA (Molecular Devices; Wokingham, UK), where addition of receptor agonists was made and fluorescence measured over time.

Measurement of surface expression of human CCR4 on recombinant cells. Surface expression of CCR4 was monitored by using a phytoerythrin-tagged antibody that was specific for the N-terminus of the receptor (R&D Systems, Abingdon, UK); a similarly tagged IgG controlled for non-specific antibody binding. CCR4-CHO cells were incubated overnight at 4 °C with the antibody in PBS supplemented with 0.1% (w/v) BSA and 10 mM sodium azide, to block antibody internalisation. Cells were then incubated in 1% (w/v) paraformaldehyde (CellFix, BD Biosciences) for 30 min before washing once and then re-suspending in incubation buffer for analysis by flow cytometry

MOL 39321

on an FC500 machine (Coulter, High Wycombe, UK). Intact cells were identified by their forward- and side-scatter characteristics and median fluorescence was measured at 575 nm using the standard FL2 channel on the device. In experiments that looked at the effect of CCR4 ligands on surface expression, cells were first incubated with increasing concentrations of CCL22 in either the absence or presence of single increasing concentrations of a CCR4 antagonist for 60 min in binding buffer at 37 °C. Cells were chilled to 4 °C before labeling with antibody as described above.

Data analysis. All data were analyzed by using GraphPad Prism (v 4.01) where concentration-effect curves typically were fitted to a four-parameter logistic equation, unless otherwise indicated. When appropriate, an F-test within Prism was used to determine significant differences in fitting parameters.

MOL 39321

Results

Functional antagonism of CCR4 responses in recombinant cells. Compounds of the pyrazinyl-sulfonamide series demonstrated no agonist activity of their own across a range of functional assays for CCR4 (data not shown), but antagonized cellular responses to CCR4 activation by either agonist. Antagonism of CCL22-mediated calcium-signaling in CCR4-HEK cells (with the agonist at a concentration equivalent to 2-3 x EC₅₀ for this response) is shown in Figure 3 for two representatives from this series, along with a structurally distinct CCR4 antagonist, BMS-397 (Compound **16** in Purandare and Somerville, 2006; see structure in Fig 1); similar results were obtained for antagonism of responses to CCL17 (data not shown).

Inhibition of agonist binding to CCR4 in recombinant cells. Incubation of adherent CCR4-CHO cells with the fluorescently labeled FB-CCL22 resulted in a time- and concentration-dependent increase in cell-associated fluorescence at room temperature. No binding of FB-CCL22 was detectable above background when using CHO cells either not expressing CCR4 or else expressing other chemokine receptors (e.g., CCR3 or CXCR2; data not shown). Cellular association of FB-CCL22 appeared to reflect a combination of binding of the labeled agonist to CCR4 along with an irreversible uptake of the fluorescent label, presumably as internalized ligand, which proceeded at a rate that varied between experiments; a typical association curve is shown in Figure 4a, which shows that in this experiment a steady-state was approached after about 3 h. If a saturating concentration (100 x estimated EC₅₀ or IC₅₀ for calcium-signaling) of either unlabeled CCL22 or a representative pyrazinyl-sulfonamide CCR4 antagonist was added at that time, then a time-dependent decrease in cell-associated fluorescence was

MOL 39321

observed (Fig 4a). These results demonstrated that this assay could be used to measure reversible agonist binding, where the data are consistent with either competition or negative co-operativity by either ligand with the fluorescent probe at the receptor and its dissociation from the cell. Dissociation of FB-CCL22 from CCR4-CHO cells by either the agonist or the antagonist proceeded to a similar degree of residual fluorescence above background after 400 min, which was assumed to represent internalized FB-CCL22 following its binding to CCR4. Binding of FB-CCL22 to CCR4-CHO cells was completely blocked by prior incubation with 1 μ M Compound **2**, and after 3 h incubation in the absence of the antagonist appeared to be saturable, with an estimated K_d of 0.6 ± 0.24 nM (Fig 4b). When measured at 3 h after simultaneous addition with the fluorescently labeled agonist (at a concentration equivalent to $2 \times K_d$), CCR4 antagonists inhibited the association of FB-CCL22 with CCR4-CHO cells in a concentration-dependent manner, with a pIC_{50} that was consistent with their activity as antagonists of CCR4-mediated calcium-signaling. Data for two representative pyrazinyl-sulfonamides and BMS-397 are shown in Figure 4c.

Binding of a radiolabeled pyrazinyl-sulfonamide to CCR4. To study the mechanism of action of the pyrazinyl-sulfonamides, a binding assay was established with a radiolabeled representative of the series. Binding of [3 H]Cmpd-1 to CCR4 was reversible and linear with increasing amounts of CCR4-expressing material (data not shown). Non-specific binding of [3 H]Cmpd-1 to CCR4-expressing cells, defined as binding in the presence of 10 μ M Compound **2**, was linear with the concentration of the radioligand (Fig 5a). Specific binding of [3 H]Cmpd-1 was saturable at equilibrium, with an estimated K_d that was consistent with the potency of unlabeled Compound **1** in a

MOL 39321

functional assay (Fig 5a). This estimated K_d at CCR4 was identical when measured by using either intact cells (either HEK or CHO) or their membrane fractions. Binding of this radioligand appeared to be specific for CCR4, in that it was not detected either in the absence of CCR4 expression or with identical host cells where other recombinant chemokine receptors were expressed (e.g., CCR3 or CXCR2; data not shown). All pyrazinyl-sulfonamides competed for binding of [3 H]Cmpd-1 to CCR4 with an estimated pIC_{50} that was consistent with their measured activity to inhibit CCR4-mediated functional responses or agonist binding to CCR4. The data for representative pyrazinyl-sulfonamide antagonists is shown in Figure 5b, along with the structurally distinct CCR4 antagonist, BMS-397, which appeared not to compete for this pyrazinyl-sulfonamide-binding site on CCR4. Interestingly, whereas unlabeled Compound 1 competed for labeled agonist binding (see Fig 4b), the binding of [3 H]Cmpd-1 to CCR4 expressed in either membranes or cells was not inhibited by unlabeled, BSA-free CCL22 and CCL17 at concentrations in excess of 10000-x their estimated K_d (data not shown).

Discordance between cellular and membrane potency at CCR4. Potency of these pyrazinyl-sulfonamide antagonists typically was independent of whether it was measured with either a membrane- or a cell-based method, using either a functional response or binding with either labeled agonist or antagonist as the probe. This structure-activity relationship is shown in the top panel of Figure 6, which correlates the pIC_{50} for inhibition of binding of FB-CCL22 to CCR4 in cells and of [3 H]Cmpd-1 to membranes and demonstrates that over a wide range of activities most compounds in this series show an excellent correspondence for cell- and membrane-based potencies. Some compounds, however, either appeared to have much lower potency in cellular

MOL 39321

assays than expected or else the cellular potency was much higher than that measured in a membrane assay. Two examples of this discordance, highlighted as open symbols in that correlation, are represented by an ester, Compound **9**, and its carboxylic acid analogue. Both compounds had identical potency in the membrane-binding assay, consistent with the structure-activity relationship of this chemical series, and yet the average pIC_{50} for ester-containing Compound **9** was significantly higher (~10-fold, $p < 0.01$) in the cell-based assay compared with the membrane-based assay (Fig 6b; Table 1). A smaller, but significant difference was seen with another ester, Compound **10** ($p < 0.01$, Table 1). In contrast, the pIC_{50} for the carboxylic acid derivative of Compound **9** was significantly lower (~100-fold, $p < 0.01$) in the cell-based assay (Fig 6b; Table 1).

Requirement for equilibration of pyrazinyl-sulfonamides across cell membranes.

The results suggested that equilibration across the cell membrane might be an issue for those antagonists that displayed these properties. Consistent with that hypothesis, the discordance in cell and membrane potency of either the ester or the carboxylic acid antagonists was eliminated by permeabilizing the cells with a low concentration (0.05% w/v) of saponin (Fig 6b; Table 1). No significant difference in the pIC_{50} was calculated for the same compounds tested in the presence of saponin. It is noteworthy that this saponin treatment revealed that some relatively impermeable compounds could even differentiate a degree of heterogeneity in what could be viewed as vesicle integrity in a membrane preparation, when binding curves appear to represent a mixture of cell potency in the presence or absence of saponin (see data for the carboxylic acid derivative of Compound **9** in Figure 6b). Permeabilization with saponin did not influence

MOL 39321

the binding of the majority of compounds in this chemical series (represented by Compound **5** in Table 1), including [³H]Cmpd-1 (data not shown).

Parallel investigation revealed, in contrast to what was observed with a typical pyrazinyl-sulfonamide, that not only were the ester-containing compounds showing higher than expected cellular activities, their activity to inhibit binding of [³H]Cmpd-1 to CCR4-CHO cells actually increased with time of incubation. This is represented by the ester Compound **10**, when measuring a time-course for inhibition of binding of [³H]Cmpd-1 to CCR4-CHO cells (Fig 7a). To explore this further, specific binding of [³H]Cmpd-1 was measured after incubation of CCR4-CHO cells with 100 nM CCR4 antagonist for 2 h followed by extensive washing of the cells. Whereas this procedure completely reversed inhibition of binding by Compound **2**, marked inhibition of binding was still observed with Compound **10**. That residual inhibition was reversed, however, by permeabilization of the cells with a low concentration (0.05% w/v) of saponin (Fig 7b). This result suggested that ester-containing compounds somehow were accumulating in the cells. Chemical analysis of CCR4-CHO cells that had been incubated for 3 h with Compound **10** revealed that there was a loss of the ester form and an accumulation of the corresponding carboxylic acid, indicating that the ester-containing compound had been hydrolyzed and retained as the poorly permeable carboxylic acid, active at CCR4, inside the cells (data not shown).

Apparent cellular activity of antagonists at CCR4 depend on properties of host cell. Binding activity at CCR4 in cell-based assays was independent of the nature of the host cell for the majority of pyrazinyl-sulfonamide antagonists, and yet the apparent activity for some compounds was significantly different when comparing the pIC₅₀ to

MOL 39321

inhibit binding at CCR4 expressed in CHO and HEK-Gq_{i5} cells and how those estimates related to the membrane assay. Whilst no significant difference in pIC₅₀ was measured between either cell- or membrane-based assays for the typical pyrazinyl-sulfonamide, Compound **2**, a significant difference in the pIC₅₀ between CHO cell and HEK-Gq_{i5} cell assays was calculated for Compound **6** at CCR4, neither estimate being comparable to the estimated membrane potency ($p < 0.001$, Table 2). The pIC₅₀ calculated for Compound **8** at CCR4 in the CHO cell assay was significantly different to that measured at CCR4 in either HEK-Gq_{i5} cells or CHO membranes ($p < 0.001$, Table 2). Preliminary attempts with the inhibitors probenecid or verapamil to explore a role for either an organic acid transporter or P-glycoprotein as the basis for this host cell dependency in compound activity failed to reveal any effect on compound binding to CCR4-CHO cells (data not shown).

Functional antagonism of agonist-mediated CCR4 internalization. To explore further the mechanism of action of these compounds, which appeared from previous evidence to require access to the cytoplasm, a robust functional assay was developed to monitor competitive antagonism – something not possible with the hemi-equilibrium conditions of the calcium-signaling assay. As described in the literature (Mariani et al., 2004), CCL22 promoted a rapid, dose-dependent disappearance of CCR4 from the surface of recombinant CHO cells, with a potency identical to that measured in other functional assays (Fig 8). Antagonism of this effect with pyrazinyl-sulfonamide antagonists at concentrations up to 1000-x their binding potency showed the expected dextral shift of the agonist dose-response curve, but a Schild analysis revealed that this effect deviated from that expected for classical competitive antagonism, especially

MOL 39321

apparent at high concentrations. Data for the representative Compound **2** are shown in Figure 8, where the fitted slope factor was significantly different from 1 ($p < 0.05$). Control experiments showed that these compounds had no effect on the specific binding of the antibody that was used to monitor surface expression of the receptor (data not shown).

Parallel structure-activity relationship for antagonists at CCR5. During the evaluation of the pyrazinyl-sulfonamides as CCR4 antagonists it was discovered that the compounds were also weaker antagonists at the chemokine receptor CCR5. These compounds reversibly inhibited FB-CCL5 binding to CCR5-CHO cells with a structure-activity relationship similar to that measured for inhibition of FB-CCL22 binding to CCR4-CHO cells, but at ~50-fold lower potency (see below in Fig 10b). It was on this basis that further biochemical work was performed to explore the potential intracellular site of action at both receptors.

Generation of C-terminal chimeras of CCR4 and CCR5. We generated recombinant HEK-Gq_{i5} cells expressing chimeric CCR4 with the C-terminal tail of CCR5 (CCR4-5T) and chimeric CCR5 with the C-terminal tail of CCR4 (CCR5-4T) (see Fig 2), to then compare their properties to the wild type receptors. When assessed within 48 h of transient expression, both of the C-terminal chimeras were expressed on the cell surface to a magnitude that appeared to be equivalent to wild type CCR4 and CCR5, as measured with relevant antibodies by using flow cytometry (data not shown).

Agonist activity of C-terminal chimeras of CCR4 and CCR5. Following transient transfection in HEK-Gq_{i5} cells, successful expression and functionality of each of the chimeras of CCR4 and CCR5 (CCR4-5T and CCR5-4T) were confirmed by measuring

MOL 39321

agonist-mediated calcium-signaling, compared in parallel studies to the wild type form of the receptors. Responses of CCR4-5T were of a similar magnitude to that observed for CCR4; the normalized dose response curves for both CCL17 and CCL22 are shown in Figure 9a. Whereas the EC_{50} for CCL17 at CCR4 was not altered by the presence of the C-terminal tail of CCR5, that for CCL22 was reduced significantly (~3-fold, $p < 0.001$) at CCR4-5T.

Responses of CCR5 expressed with the C-terminal tail of CCR4 (CCR5-4T) to either CCL4 or CCL5 were variable, but usually markedly attenuated from that observed for wild type CCR5, both in terms of the overall magnitude of the response and the potency of the agonist; normalized dose response curves for both CCL4 and CCL5 are shown in Figure 9b. Assuming that the dose-response curves did not deviate from a simple rectangular hyperbola, then if all data were analyzed assuming a common slope factor, the EC_{50} for CCL4 was estimated to be reduced ~5-fold at CCR5-4T ($p < 0.001$) whereas that for CCL5 was estimated to be reduced ~16-fold ($p < 0.001$), when compared to CCR5 WT.

Antagonist binding of C-terminal chimeras of CCR4 and CCR5. Saturable, high affinity binding of [3 H]Cmpd-1 was measured to cells transiently expressing wild type CCR4 ($pK_d = 8.71 \pm 0.023$, $n = 3$), but binding to the chimeric CCR4-5T was not detectable (Fig 10a). In contrast, saturable, high affinity binding of [3 H]Cmpd-1 was measured to CCR5 on cells only when expressed as a chimera with the C-terminal tail of CCR4 (CCR5-4T; Fig 10a), with a small but significant decrease in affinity ($pK_d = 8.21 \pm 0.024$, $n = 3$; $p < 0.001$ compared to wild type CCR4). In contrast to their activity at the wild type CCR5, competition by a range of pyrazinyl-sulfonamides for binding of

MOL 39321

[³H]Cmpd-1 (at a concentration equivalent to 2 x K_d) to cells expressing CCR5-4T was identical to that observed with wild type CCR4 (Fig 10b).

Antagonist activity of C-terminal chimeras of CCR4 and CCR5. In functional assays of CCR4 and CCR5 activity, the potencies of pyrazinyl-sulfonamides at CCR4 were equivalent to CCR5-4T and those at CCR5 were equivalent to CCR4-5T. The results for a representative compound to antagonize the response of CCR4 and CCR4-5T or CCR5 and CCR5-4T to CCL22 or CCL5, respectively, are shown in Figure 11a; identical results were observed for responses to CCL17 or CCL4 at CCR4 and CCR4-5T or CCR5 and CCR5-4T, respectively (data not shown). In contrast, the presence of a chimeric C-terminal domain did not affect the relative selectivity of the non-pyrazinyl-sulfonamides BMS-397 and SCH-C at CCR4 and CCR5 (Fig 11b).

MOL 39321

Discussion

Upon discovery of the pyrazinyl-sulfonamide CCR4 antagonists through a cell-based screen it was assumed that these molecules were active at an overlapping extracellular site for the chemokine ligands of this GPCR. The data were consistent with that interpretation. The compounds are functional antagonists at CCR4, similar in activity to another published antagonist, BMS-397, blocking calcium-signaling to CCR4 agonists. The compounds promote dissociation of an agonist from CCR4-expressing cells. Binding of pyrazinyl-sulfonamides is CCR4-dependent, reversible and appears to be to a single site on the receptor. Other compounds from this series compete for binding to this site with affinities that correlate to their functional activity, but the site is selective such that the structurally distinct BMS-397 does not appear to compete for binding. Additional data, however, demonstrate that the pyrazinyl-sulfonamides require access to the cytoplasm for their activity, suggesting that these antagonists act via an intracellular site on CCR4. This novel finding is supported by a series of observations that relate to the property of a compound to maintain an intracellular concentration in steady-state with the extracellular medium. The cell plasma membrane appeared to present a diffusion barrier for some compounds from this chemical series, which showed a significant decrease in cell potency when compared to their activity in a membrane assay. This explanation also would account for the measured time-dependent increase in apparent cell potency of ester-containing compounds, as these crossed the plasma membrane but were then hydrolyzed and accumulated within cells as the poorly permeable, but active carboxylic acid. Those differential cell binding potencies were eliminated by incubation of the recombinant cells with a low

MOL 39321

concentration of saponin, a common method to permeabilise, but not solubilise, the cell plasma membrane (Brooks and Treml, 1983) and which allows otherwise poorly permeable molecules to equilibrate across the plasma membrane. Whilst it is possible that the saponin treatment might simply have altered membrane fluidity through complexation with cholesterol, perhaps allowing compounds better access to an extracellular site in the context of an intact cell, this is not consistent with the other data. For example, the dependency of compound binding potency on the host cell background for CCR4 expression (Table 2) is consistent with the knowledge that intracellular steady-state compound concentrations will depend on the host cell's complement of drug transporters, with their different substrate specificities (e.g., P-glycoprotein or the ATP-binding cassette family) that will differ in profile between cell types (Kim, 2006); further work could establish the relevant process. Finally, in support of the conclusion that the pyrazinyl-sulfonamides bind intracellularly and hence cannot act competitively, their functional antagonism suggests non-competitiveness or negative co-operativity, as also would be concluded from their effect to promote agonist dissociation.

The parallel structure-activity relationship for the pyrazinyl-sulfonamides at both CCR4 and CCR5 infers a similar mechanism of action at conserved points of interaction, such that these receptors might share significant homology in the region of this proposed binding site¹. This idea, taken together with the evidence that these compounds appear to require access to an intracellular site on the receptor, suggested that the contribution of different intracellular domains of CCR4 and CCR5 to the interaction of these compounds should be considered. A first simple approach was to explore the

MOL 39321

contribution of the C-terminal region to compound activity, encompassing everything beyond the highly conserved GPCR motif, NPxxY (Fritze et al., 2003) in the modeled extracellular half of TM7, including Helix 8 (see Figure 2).

Swapping the C-terminal domains between CCR4 and CCR5 resulted in chimeras (CCR5-4T and CCR4-5T) that were highly expressed in recombinant cells and functionally coupled to calcium-signaling, albeit with reduced agonist potency at either receptor apart from the activity of CCL17 at CCR4 and CCR4-5T. This differential effect for CCR4 agonist potency at CCR4-5T may be related to the differential ability of CCL17 and CCL22 to promote receptor internalization (Mariani et al., 2004), which has been shown for other GPCRs to involve the C-terminus (Bockaert et al., 2003). Similarly, an attenuated response and potency of CCL4 and CCL5 at CCR5-4T either could reflect a limited degree of effective receptor expression and receptor reserve for signaling or perhaps highlight a role for the integrity of the C-terminus in CCR5 signaling, at least through calcium, in a recombinant cell. Notwithstanding these effects on agonist responses it was still possible to compare the effects and interactions with the pyrazinyl-sulfonamide-binding site of the antagonists between the wild type and chimeric receptors. The most significant result from that comparison is that potent binding and antagonist activity of the pyrazinyl-sulfonamides appear to depend on which C-terminal portion was expressed. The overall structure-activity relationship is independent of the nature of the C-terminal domain, but the presence of the C-terminal domain from CCR4 accounts for the parallel 50-fold increase in compound potency over CCR5 (see Figure 10b). The presence of different C-terminal domains does not affect the selectivity of the structurally distinct antagonists, BMS-397 and SCH-C, which do not compete for binding

MOL 39321

to the site labeled by a pyrazinyl-sulfonamide and so must bind elsewhere on the receptors.

The most likely explanation for the non-competitive functional antagonism, promotion of agonist dissociation from the receptor and the requirement for intracellular access is that these pyrazinyl-sulfonamide antagonists bind to an allosteric site on CCR4 and CCR5, perhaps always expected for a chemokine antagonist that was so much smaller than the natural ligand, but uniquely in that the site appears to be located in a conserved intracellular region of these receptors that involves components of the C-terminal domain. The concept of allosteric interactions in GPCRs is already well appreciated for GPCRs, and numerous allosteric ligands have been described for Class A GPCRs (Christopoulos, 2002; Birdsall and Lazareno, 2005), including CCR5 (Kazmierski et al., 2005). Interaction of the pyrazinyl-sulfonamides do not, however, conform to a classical allosteric ternary complex model with the expected reciprocation between the two ligands (Birdsall and Lazareno, 2005). In recombinant systems, binding of these antagonists to this intracellular allosteric site promotes the dissociation of agonists from the receptor and so must decrease the apparent affinity of the receptor for agonists, and yet agonists do not appear to affect binding of antagonists. We have not been able to determine whether this represents an artifact of the recombinant system whereby the receptor is over-expressed relative to the concentration of G protein, to yield mutually exclusive pools of coupled and uncoupled receptors. According to the simple ternary complex model (Wreggett and De Lean, 1984) such a situation is predicted to produce a significantly lower amount of high affinity agonist-binding relative to that observed for antagonists, but we have no evidence to suggest

MOL 39321

that this model is even applicable. It is also possible that these interactions might reflect co-operativity between monomers of an oligomeric complex, as has been described for GPCRs (Wreggett and Wells, 1995; Springael et al., 2005). The nature of this proposed allosteric interaction will be the subject of further work.

Future work will also be important to identify the location of this intracellular site. Although the sites of allosteric interaction on a Class A GPCR have not yet been identified, since this work was completed a theoretical model has suggested a potential intracellular pocket in the region of TM2 and Helix 8 of the M₁-muscarinic receptor (Espinoza-Fonseca and Trujillo-Ferrara, 2006). That proposal would be consistent with our experimental data, with the predicted Helix 8 being contained within the C-terminal domain used to support the existence of this intracellular, allosteric site. The C-terminal domain of GPCRs in the region of Helix 8 has been identified as a key area for interaction with G proteins, critical for coupling of the receptor to G protein activation (Krishna et al., 2002; Lu et al., 2002; Delos Santos et al., 2006; Lehmann et al., 2007), as well as with arrestins, which can be important for activation-mediated GPCR internalization or secondary signaling (Bockaert et al., 2003).

Given the selective activity of the pyrazinyl-sulfonamides as a particular class of antagonists at both CCR4 and CCR5, along with the high degree of conservation of this C-terminal region of GPCRs, it would be important to establish whether this is a generic feature of this class of molecular targets that could be used for novel drug discovery. Antagonists acting through this mechanism would provide an approach that may offer advantages and novelty over existing therapies. For example, such antagonists of chemokine receptors (e.g., CCR5) might provide an effective means to block viral entry.

MOL 39321

This work has a significant impact on the choice of methods for screening for novel compounds and rational drug design. Cell-based assays could miss chemical leads if those early compounds did not have the necessary properties to equilibrate across cell membranes; within a chemical series such compounds could generate misleading structure-activity relationships. An unfortunate choice of host cell for expression of a recombinant GPCR could have the same effect if pumps or transporters influence the effective intracellular concentration. Localization of this novel binding-site will allow for the development of new molecular models and screening methods that can aid discovery of novel drugs.

MOL 39321

Acknowledgments

David Wilkinson (Department of Medicinal Chemistry, AstraZeneca R&D) provided [³H]Cmpd-1. Nicholas Kindon, Rhona Cox, Barry Teobald, James Reuberson, Bryan Roberts, Tim Luker, Antonio Mete, Richard Harrison, Tim Johnson and Alan Faull (Department of Medicinal Chemistry, AstraZeneca R&D) synthesized the chemokine antagonists used in this study. We thank Nicholas Tomkinson for his analysis of GPCR homology models, and Caroline Grahames and John Unitt for critical review of the manuscript. Dr Ashok Purandare (Bristol-Myers Squibb) kindly revealed the specific name for the BMS compound used in this study.

MOL 39321

References

Ajuebor MN, Carey JA and Swain MG (2006) CCR5 in T-cell mediated liver diseases: What's going on?. *J Immunol* **177**:2039-2045.

Baxter A; Johnson T, Kindon N, Roberts B, Steele J, Stocks, M, Tomkinson N (2003a) Preparation of N-pyrazinylthiophenesulfonamides as chemokine receptor modulators. *PCT WO* 2003051870.

Baxter A; Johnson T, Kindon N, Roberts B, Stocks, M (2003b) Preparation of N-pyrazinylbenzenesulfonamides as their use in the treatment of chemokine mediated diseases such as asthma. *PCT WO* 2003059893.

Baxter A; Kindon N, Stocks, M (2005) Preparation of condensed N-pyrazinyl-sulfonamides as their use in the treatment of chemokine mediated diseases. *PCT WO* 2005021513.

Biophoenix (2005) *The Emerging Drug Targets Outlook: An analysis of novel molecular targets to develop innovative new therapeutics*. Business Insights, www.BI-Interactive.com

Birdsall NJM and Lazareno, S (2005) Allosterism at muscarinic receptors: Ligands and mechanisms. *Mini Rev Med Chem* **5**:523-543.

Bockaert J, Marin P, Dumuis A and Fagni L (2003) The 'magic tail' of G protein-coupled receptors: An anchorage for functional protein networks. *FEBS Lett* **546**:65-72.

Brooks JC and Trembl S (1983) Catecholamine secretion by chemically skinned cultured chromaffin cells. *J Neurochem* **40**:468-473.

Christopoulos, A (2002) Allosteric binding sites on cell-surface receptors: Novel targets for drug discovery. *Nat Rev Drug Disc* **1**:198-210.

MOL 39321

Delos Santos NM, Gardner LA, White SW and Bahouth SW (2006) Characterization of the residues in helix 8 of the human β_1 -adrenergic receptor that are involved in coupling the receptor to G proteins. *J Biol Chem* **281**:12896-12907.

Devereux J, Haeberli P and Smithies O (1984) A comprehensive set of sequence analysis programs for the VAX. *Nucl Acids Res* **12**:387-395.

Espinoza-Fonseca LM and Trujillo-Ferrara JG (2006) The existence of a second allosteric site on the M₁ muscarinic acetylcholine receptor and its implications for drug design. *Bioorg Med Chem Lett* **16**:1217-1220.

Ferenczi K, Fuhlbrigge RC, Pinkus JL, Pinkus GS and Kupper TS (2002) Increased CCR4 expression in cutaneous T cell lymphoma. *J Invest Derm* **119**:1405-1410.

Fritze O, Filipek S, Kuksa V, Palczewski K, Hofmann KP and Ernst OP (2003) Role of the conserved NPxxY(x)_{5,6}F motif in the rhodopsin ground state and during activation. *Proc Nat Acad Sci* **100**:2290-2295.

Haringman JJ, Kraan MC, Smeets TJM, Zwinderman KH and Tak PP (2003) Chemokine blockade and chronic inflammatory disease: Proof of concept in patients with rheumatoid arthritis. *Ann Rheum Dis* **62**:715-721.

Homey B, Steinhoff M, Ruzicka T and Leung DYM (2006) Cytokines and chemokines orchestrate atopic skin inflammation. *J Allerg Clin Immunol* **118**:178-189.

Ishida T and Ueda R (2006) CCR4 as a novel molecular target for immunotherapy of cancer. *Cancer Sci* **97**:1139-1146.

Horton RM, Hunt HD, Ho SN, Pullen JK and Pease LR (1989) Engineering hybrid genes without the use of restriction enzymes: gene splicing by overlap extension. *Gene* **77**:61-68.

MOL 39321

Johnson Z, Power CA, Weiss C, Rintelen F, Ji H, Ruckle T, Camps M, Wells TNC, Schwartz MK, Proudfoot AEI and Rommel C (2004) Chemokine inhibition – why, when, where, which and how? *Biochem Soc Trans* **32**:366-377.

Kazmierski W, Bifulco N, Yang H, Boone L, DeAnda F, Watson C and Kenakin, T (2003) Recent progress in discovery of small-molecule CCR5 chemokine receptor ligands as HIV-1 inhibitors. *Bioorg Med Chem* **11**:2663-2676.

Kim RB (2006) Transporters and drug discovery: Why, when and how. *Mol Pharmaceut* **3**:26-32.

Krishna AG, Menon ST, Terry TJ and Sakmar TP (2002) Evidence that helix 8 of rhodopsin acts as a membrane-dependent conformational switch. *Biochem* **41**:8298-8309.

Kristiansen K (2004) Molecular mechanisms of ligand binding, signaling, and regulation within the superfamily of G-protein-coupled receptors: molecular modeling and mutagenesis approaches to receptor structure and function. *Pharmacol Therapeut* **103**:21-80.

Lehmann N, Alexiev U and Fahmy K (2007) Linkage between the intramembrane H-bond network around aspartic acid 83 and the cytosolic environment of helix 8 in photoactivated rhodopsin. *J Mol Biol* **366**:1129-1141.

Lu Z-L, Saldanha JW and Hulme EC (2002) Seven-transmembrane receptors: crystals clarify. *Trends Pharm Sci* **23**:140-146.

Mariani M, Lang R, Binda E, Panina-Bordignon P and D'Ambrosio D (2004) Dominance of CCL22 over CCL17 in induction of chemokine receptor CCR4 desensitization and internalization on human Th2 cells. *Eur J Immunol* **34**:231-240.

MOL 39321

Mellentin-Michelotti J, Evangelista LT, Swartzman EE, Miraglia SJ, Werner WE and Yuan P-M. (1999) Determination of ligand binding affinities for endogenous seven-transmembrane receptors using fluorometric microvolume assay technology. *Analyt Biochem* **272**:182-190.

Palani A, Shapiro S, Clader JW, Greenlee WJ, Cox K, Strizki J, Endres M and Baroudy BH (2001) Discovery of 4-[(Z)-(4-bromophenyl)-ethoxyimino)methyl]-1'-[(2,3-dimethyl-3-pyridinyl)carbonyl]-4'-methyl-1,4'-bipiperidine-*N*-oxide (SCH 351125): An orally bio-available human CCR5 antagonist for the treatment of HIV infection. *J Med Chem* **44**:3339-3342.

Palczewski K, Kumasaka T, Hori T, Behnke, CA, Motoshima H, Fox BA, Le Trong I, Teller DC, Okada T, Stenkamp RE, Yamamoto M and Miyano M (2000) Crystal structure of rhodopsin: A G Protein-Coupled Receptor. *Science* **289**:739-745.

Panina-Bordignon P, Papi A, Mariani M, Di Lucia P, Casoni G, Bellettato C, Buonsanti C, Miotto D, Mapp C, Villa A, Arrigoni G, Fabbri LM and Sinigaglia F (2001) The C-C chemokine receptors CCR4 and CCR8 identify airway T cells of allergen-challenged atopic asthmatics. *J Clin Invest* **107**:1357-1364.

Prahalad S (2006) Negative association between the chemokine receptor CCR5-Delta32 polymorphism and rheumatoid arthritis. *Genes Immun* **7**:264-268.

Proudfoot AE (2002) Chemokine receptors: Multifaceted therapeutic targets. *Nat Rev Immunol* **2**:106-115.

Purandare AV (2004) Preparation of piperazines as chemokine receptor antagonists. *PCT WO* 2004020584

MOL 39321

Purandare AV and Somerville JE (2006) Antagonists of CCR4 as immunomodulatory agents. *Curr Top Med Chem* **6**:1335-1344.

Saeki T (2004) Small-molecule chemokine receptor antagonists: Potential targets for inflammatory and allergic disorders. *Curr Med Chem – Anti-Inflam Anti-Aller Agents* **3**:363-375.

Schertler GFX (2005) Structure of rhodopsin and the metarhodopsin I photointermediate. *Cur Opin Struc Biol* **15**:408-415.

Schuh JM, Power CA, Proudfoot AE, Kunkel SL, Lukacs NW and Hogaboam (2002) Airway hyperresponsiveness, but not airway remodeling, is attenuated during chronic pulmonary allergic responses to *Aspergillus* in CCR4^{-/-} mice. *FASEB J* **16**:1313-1315.

Springael J-Y, Urizar E and Parmentier M (2005) Dimerization of chemokine receptors and its functional consequences. *Cyt Growth Fact Rev* **16**:611-623.

Wreggett KA and De Lean A (1984) The ternary complex model: Its properties and application to the D₂-dopamine receptor of the bovine anterior pituitary gland. *Mol Pharmacol* **26**:214-227.

Wreggett KA and Wells JW (1995) Cooperativity manifest in the binding properties of purified cardiac muscarinic receptors. *J Biol Chem* **270**:22488-22499.

MOL 39321

Footnotes

[†]Author for correspondence: Dr Keith Wreggett, Department of Discovery BioScience, AstraZeneca R&D Charnwood, Bakewell Road, Loughborough, Leicestershire, UK, LE11 5RH. Email: Keith.Wreggett@astrazeneca.com

¹Protein sequence identity between human CCR4 and CCR5 is ~50% overall, about average across the CC chemokine receptors. If an arbitrary line was drawn through an homology model of CCR4 at the midpoint of the longitudinal axis of the predicted transmembrane domains then extracellular and intracellular identity between the two receptors is estimated at 45% and 53%, respectively.

MOL 39321

Figure Legends

Figure 1 Structure of CCR4 and CCR5 antagonists used in this study

Figure 2 Construction of the CCR4 and CCR5 chimeras. Alignment of the C-terminal section of protein sequences for human CCR4 and CCR5 were generated using the UWGCG GAP program (Devereux et al., 1984). The predicted transmembrane domain VII is shown in bold type. The region of high homology between the two sequences, including the conserved NPxxY motif, is shown boxed. Primers for splice overlap extension (SOE) PCR were designed to cover this region. Those primer sequences were:

CCR4for: CGGAATTCAAGCTTCCACCATGAACCCACGGATATAGC

CCR4rev: GATCTTCATGATGCTCTGTAGGCGGCCGCTAGC

CCR5for: ATCTGCTAGCCACCATGGATTATCAAGTGTCAAGT

CCR5rev: ATCTGCGGCCGCTCACAAGCCCACAGATATTT

TM7for: CACTGCTGCCTIAATCCCATCATCTA

TM7rev: TAGATGATGGGATTAAGGCAGCAGTG

The TM7for/rev primers corresponding to the region of overlap were used on both CCR4 and CCR5 templates. The primers matched perfectly with the CCR4 template and had two mismatches with CCR5 (underlined). TM7for and TM7rev were complementary to one another; amplification of fragments using these primers generated the 26bp regions of overlap necessary for the SOE PCR.

MOL 39321

Figure 3 Antagonism of CCR4 functional activity in recombinant cells. Calcium-signaling to 0.6 nM (2-3 x EC₅₀) CCL22 was measured at room temperature with Fluo-3 loaded HEK-Gq_{i5} cells expressing recombinant human CCR4, as described in Materials and Methods. Responses to CCR4 activation were measured in either the absence or presence of concentrations of CCR4 antagonists as shown on the *abscissa*, where compounds were pre-incubated for 15 min before addition of the agonist. The fluorescent signal at each concentration was measured in triplicate and then plotted on the *ordinate* as a percentage of the maximal response normalized to 100% of CCL22-signaling in the absence of CCR4 antagonist, after subtraction of the background signal in the absence of agonist. The data represent the average and standard error of four experiments. The *lines* represent the fit of a simple rectangular hyperbola with a slope factor of 1, constraining the top and bottom of the curves to 100 and 0, respectively. Estimates of pIC₅₀ were made for Compound 1 (*closed squares*; 8.02 ± 0.067), Compound 2 (*open squares*; 7.30 ± 0.043) and BMS-397 (*closed triangles*; 7.57 ± 0.043)

Figure 4 Inhibition of agonist binding to CCR4 in recombinant cells. A. Total binding of FB-CCL22 was measured at room temperature to CHO cells expressing recombinant human CCR4, over the period of time shown on the *abscissa*, in the absence or presence of 10 μM Compound 2 to measure non-specific binding. Non-specific binding was subtracted from total binding to give specific binding (*closed circles*), which was plotted in relative fluorescence units on the *ordinate*. Addition (indicated by the *arrow*) of buffer in the absence or presence of either a CCR4

MOL 39321

antagonist 10 μ M Compound **2** (*open square*) or 100 nM unlabeled CCL22 (*open circles*) was made after 2 h pre-incubation with FB-CCL22 at room temperature, and cell-associated fluorescence was measured over a further 260 min. The *lines* simply link the data points. **B.** Total (*closed squares*) and non-specific (in the presence of 10 μ M Compound **2**; *open squares*) binding of FB-CCL22 to CHO cells expressing recombinant human CCR4 was measured at concentrations as indicated on the *abscissa*, following incubation of the receptor for 2 h at room temperature. The data represent the average and standard deviation of three separate experiments. The *lines* either connect the data points (total binding) or represent the best fit of a linear regression (non-specific binding). Specific binding was calculated as total binding subtracting the corresponding non-specific binding (data not shown). **C.** Total binding of FB-CCL22 to CHO cells expressing recombinant human CCR4 was measured, following incubation of the receptor with 0.7 nM FB-CCL22 for 3 h at room temperature. Binding was measured in either the absence or presence of concentrations of CCR4 antagonists as shown on the *abscissa*. Specific binding was calculated as described in **A** and plotted on the *ordinate* as a percentage of maximum specific FB-CCL22 binding in the absence of CCR4 antagonist. The data represent the average and standard error of four experiments. The *lines* represent the fit of a simple rectangular hyperbola with a slope factor of 1, constraining the top and bottom of the curves to 100 and 0, respectively.. Estimates of pIC_{50} were made for Compound **1** (*closed squares*; 8.36 ± 0.067), Compound **2** (*open squares*; 7.68 ± 0.053) and BMS-397 (*closed triangles*; 7.81 ± 0.051).

MOL 39321

Figure 5 Binding of CCR4 antagonists to recombinant CCR4 expressed in membranes. Left Panel. Total binding of [³H]Cmpd-1 to CCR4-CHO membranes was measured at room temperature. The radioligand was incubated at concentrations as shown on the *abscissa*, in the absence or presence of a saturating concentration of an unlabeled pyrazinyl-sulfonamide (differing between some experiments) to measure non-specific binding. Non-specific binding was subtracted from total binding to give specific binding that was then normalized to 100% of maximum and plotted on the *ordinate*. The data represent the average and standard error of four experiments. The *line* represents the fit of a simple rectangular hyperbola with a slope factor of 1. The pK_d was estimated at 8.50 ± 0.010 (K_d = 3 nM). **Inset.** Total and non-specific binding from one of the four experiments is shown. Radioactivity bound to membranes in either the presence (*open squares*) or absence (*closed triangles*) of a pyrazinyl-sulfonamide CCR4 antagonist was plotted on the *ordinate*. **Right Panel.** Competition for the specific binding of 1 nM [³H]Cmpd-1 was measured for the CCR4 antagonists Compound 1 (*closed squares*), Compound 2 (*open squares*) and BMS-397 (*closed triangles*), following equilibration with membranes from CCR4-CHO cells at room temperature. Compounds were tested in duplicate, at concentrations plotted on the *abscissa*. Specific binding was calculated as described in the **Left Panel** and plotted on the *ordinate* as a percentage of specific [³H]Cmpd-1 binding alone. The data represent the average and standard error of four experiments. The *lines* for the first two compounds represent the fit of a simple rectangular hyperbola with a slope factor of 1, constraining the value of the top and bottom of the curves to 100 and 0, respectively.

MOL 39321

The *dashed line* for BMS-397 simply connects the data points. Estimates of pIC₅₀ were made for Compound **1** (8.75 ± 0.038) and Compound **2** (7.70 ± 0.041)

Figure 6 Correlation of CCR4 antagonist activity in cell- and membrane-based assays and the effect of saponin permeabilization. Top panel. Activities were compared for a wide range of a pyrazinyl-sulfonamide CCR4 antagonists (256 compounds) between inhibition of FB-CCL22-binding to CCR4-CHO cells (Cellular Potency) and inhibition of [³H]Cmpd-1-binding to membranes from CCR4-CHO cells (Membrane Potency). For estimates of cellular potency, total binding of 0.7 nM FB-CCL22 was measured after 2 h incubation in the absence and presence of at least five concentrations of a CCR4 antagonist, and the pIC₅₀ estimated as described in Materials and Methods. Average pIC₅₀ data calculated from at least two experiments were plotted on the *abscissa*. CCR4-CHO membrane-binding activity was measured by competition for the specific binding of 1 nM [³H]Cmpd-1 in the absence and presence of at least five concentrations of a CCR4 antagonist, following incubation with CCR4-CHO membranes for 1 h at room temperature, and the pIC₅₀ estimated as described in Materials and Methods. Average pIC₅₀ data calculated from at least two experiments were plotted on the *ordinate*. Highlighted on this graph are the positions in the correlation for the ester-containing Compound **9** (*open triangle*) and its carboxylic acid derivative (*open circle*), with the *arrows* pointing to the relevant structural group and associated data. Competition for the specific binding of 1 nM [³H]Cmpd-1 was measured for either Compound **9** (**Bottom Right Panel**) or its carboxylic acid derivative (**Bottom Left Panel**) at concentrations shown on the *abscissa*, following equilibration

MOL 39321

with CCR4-CHO cells in the presence (*open circles*) or absence (*closed circles*) of 0.05% (w/v) saponin or with CCR4-CHO membranes (*closed squares*). Specific [³H]Cmpd-1 binding was plotted on the *ordinate* as a percentage of that in the absence of competing ligand. The data represent the average and standard error of either three or four experiments. The *lines* represent the fit of a simple rectangular hyperbola with a slope factor of 1, constraining the value of the top and bottom of the curves to 100 and 0, respectively. Estimates of pIC₅₀ for binding of both compounds to either CCR4-CHO cells or membranes ± 0.05% (w/v) saponin are presented in Table 1. Data for binding of the carboxylic acid derivative to CCR4-CHO membranes were fitted to a two-site model, represented by the *dashed line*; with estimates of pIC₅₀ for the first site (fraction = 70%) and second site were 8.0 ± 0.11 and 6.1 ± 0.26, respectively.

Figure 7 Intracellular trapping of an ester-containing pyrazinyl-sulfonamide in CCR4-CHO cells and the effect of saponin permeabilization on CCR4 antagonism.

A. Inhibition of the specific binding of 1 nM [³H]Cmpd-1 to either CCR4-CHO cells (*closed circles*) or CCR4-CHO membranes (*open squares*) was measured for 10 nM Compound **10** after incubation at room temperature at time intervals as shown on the *abscissa*. Non-specific binding, defined with 10 μM Compound **2**, was subtracted from total binding to give specific binding; the percentage inhibition at each time was calculated and plotted on the *ordinate*. The data for 1-3 h incubations represent the mean and standard error of at least four experiments, or two experiments for the 20 min incubation data. Percentage inhibition significantly increased in the cell-based assay between 1 and 3 h ($p < 0.05$) with values at 2 and 3 h being significantly higher than in

MOL 39321

the membrane-based assay ($p < 0.01$). **B.** Reversibility of compound binding to CCR4 was measured in a competition assay for the specific binding of 1 nM [^3H]Cmpd-1 to CCR4-CHO cells. Compounds **2** (*white bars*) and **10** (*black bars*) were pre-incubated at 100 nM with cells for 2 h at room temperature before washing cells extensively in binding buffer. Compounds, buffer or 0.05% (w/v) saponin (*hatched bar*) was then re-added, and cells were incubated for a further 30 min following addition of 1 nM [^3H]Cmpd-1. Specific [^3H]Cmpd-1 binding was plotted on the *ordinate* as a percentage of that in the absence of a CCR4 antagonist.

Figure 8 Functional antagonism of CCL22-mediated internalization of CCR4 in recombinant CHO cells. **Left panel.** Expression of CCR4 on recombinant CHO cells was monitored by using flow cytometry to measure the labeling of surface receptor with a CCR4-specific PE-tagged antibody, as described in Materials and Methods. Agonist-mediated CCR4 internalization at 37 °C was measured at CCL22 concentrations as shown on the *abscissa*, in either the absence or presence of Compound **2** at single increasing concentrations as shown in the *legend*. A single measurement of the fluorescence signal at each concentration was measured and then plotted on the *ordinate* as a percentage of the maximal response normalized to 100% of CCL22-mediated internalization in the absence of CCR4 antagonist. The data represent one of three similar experiments. The *lines* represent the best fit of a simple rectangular hyperbola with a shared slope factor, constraining the top and bottom of the curves to 100 and 0, respectively. **Right panel.** Schild analysis of the data shown in the left panel. The *solid line* represents the best fit of a linear regression, having a slope factor

MOL 39321

of 0.71. The *dashed line* represents the predicted behavior for a competitive interaction, plotted with a slope factor of 1 and an affinity measured independently by competition with [³H]Cmpd-1.

Figure 9 Comparison of functional activity of wild type and C-terminal chimeras

of human CCR4 and CCR5 in recombinant cells. A. Calcium responses were measured in Fluo-3 loaded HEK-Gq_{i5} cells transiently expressing either wild-type (WT) CCR4 (*closed symbols*) or chimeric CCR4 with the C-terminal tail of CCR5 (CCR4-5T; *open symbols*) following addition of either CCL22 (*circles*) or CCL17 (*triangles*) at concentrations as shown on the *abscissa*. The fluorescence signal at each concentration was measured in quadruplicate and then plotted on the *ordinate* as a percentage of the maximal response normalized to 100% of maximal agonist signaling, after subtraction of the background signal in the absence of agonist. The data represent the average and standard error of either four (CCL22) or three (CCL17) experiments. The *lines* represent the best fit of a simple rectangular hyperbola, constraining the slope factor at 1 and top and bottom at 100 and 0, respectively. Estimates of pEC₅₀ for CCL22 were 9.57 ± 0.023 (EC₅₀ = 0.27 nM; CCR4 WT) and 9.13 ± 0.026 (EC₅₀ = 0.73 nM; CCR4-5T), and for CCL17 were 9.44 ± 0.039 (EC₅₀ = 0.36 nM; CCR4 WT) and 9.47 ± 0.050 (EC₅₀ = 0.33 nM; CCR4-5T). **B.** As in **A**, but measuring responses in wild-type (WT) CCR5 (*closed symbols*) or chimeric CCR5 with the C-terminal tail of CCR4 (CCR5-4T; *open symbols*) following addition of either CCL5 (*circles*) or CCL4 (*triangles*). The data represent the average and standard error of four experiments. The *lines* represent the best fit of a simple rectangular

MOL 39321

hyperbola, sharing the slope factor for all curves and constraining top and bottom at 100 and 0, respectively. The common slope factor for all curves was estimated at 1.4 ± 0.11 . Estimates of pEC_{50} for CCL5 were 9.44 ± 0.052 ($EC_{50} = 0.37$ nM; CCR5 WT) and 8.24 ± 0.052 ($EC_{50} = 5.8$ nM; CCR5-4T), and for CCL4 were 9.17 ± 0.052 ($EC_{50} = 0.67$ nM; CCR5 WT) and 8.44 ± 0.061 ($EC_{50} = 3.6$ nM; CCR5-4T).

Figure 10 A. Binding of [³H]Cmpd-1 to wild type and C-terminal chimeras of human CCR4 and CCR5 in recombinant cells. Binding of [³H]Cmpd-1 was measured at concentrations as shown on the *abscissa*, following equilibration at room temperature with HEK-Gq_{i5} cells transiently expressing either wild-type (WT) CCR4 (*closed circles*), CCR5 WT (*closed triangles*), chimeric CCR4 with the C-terminal tail of CCR5 (CCR4-5T; *open circles*) or chimeric CCR5 with the C-terminal tail of CCR4 (CCR5-4T; *open triangles*). Non-specific binding, defined by 10 μ M Compound **2**, was subtracted from total binding to give specific binding that was then normalized to 100% of maximum and plotted on the *ordinate*. The *lines* represent the best fit of a simple rectangular hyperbola with a slope factor of 1 to the pooled data of three experiments. Estimates of pK_d for the radioligand were 8.71 ± 0.020 (CCR4 WT) and 8.27 ± 0.020 (CCR5-4T). Specific binding of [³H]Cmpd-1 to CCR5 WT and CCR4-5T did not reach 50% of maximum at concentrations of 13 nM and 32 nM, respectively. **B. Correlation of antagonist binding potencies between human CCR4 and either WT or chimeric CCR5.** Inhibition of the specific binding of FB-CCL22 to CCR4-CHO cells or FB-CCL5 to CCR5-CHO cells by compounds **1**, **2**, **4**, **5** and **7** was measured following incubation of each receptor with 0.7 nM FB-chemokine in the absence or presence of a range of

MOL 39321

antagonist concentrations for 3 h at room temperature. Average pIC_{50} data calculated from four experiments were plotted as a correlation (*open squares*), with values on the *abscissa* representing the pIC_{50} measured at wild-type CCR5 and values on the *ordinate* representing the pIC_{50} measured at wild-type CCR4. Competition for the specific binding of [3H]Cmpd-1 to HEK-Gq $_{i5}$ cells expressing wild-type CCR4 and chimeric CCR5 with the C-terminal tail of CCR4 (CCR5-4T) by Compounds **1**, **2**, **4**, **5** and **7**, was measured following incubation of each receptor with 1 nM [3H]Cmpd-1 for 1 h at room temperature. The average pIC_{50} calculated from four experiments were plotted as a correlation (*closed squares*), with values on the *abscissa* representing the pIC_{50} measured at CCR5 WT and CCR5-4T and values on the *ordinate* representing the pIC_{50} measured at wild-type CCR4. The *dashed line* represents identity, while the solid lines represent the best fit of a linear regression of each correlation, with identical slope factors and differing in the intercept by a value of 50.

Figure 11. Antagonism of agonist signaling with wild type and C-terminal chimeras of human CCR4 and CCR5 in recombinant cells. Calcium responses were measured in Fluo-3 loaded HEK-Gq $_{i5}$ cells transiently expressing either wild-type (WT) CCR4 (*closed circles*), CCR5 WT (*closed triangles*), chimeric CCR4 with the C-terminal tail of CCR5 (CCR4-5T; *open circles*) or chimeric CCR5 with the C-terminal tail of CCR4 (CCR5-4T; *open triangles*). Antagonism of the response to either CCL22 (0.3 nM) or CCL5 (0.6 nM for WT and 20 or 30 nM for CCR5-4T) was measured for compounds at concentrations as shown on the *abscissa*, after pre-incubation for 15 min before addition of the agonist. The fluorescence signal at each concentration was measured in

MOL 39321

quadruplicate and then plotted on the *ordinate* as a percentage of the maximal response normalized to 100% of maximal agonist signaling, after subtraction of the background signal in the absence of agonist. The data represent the average and standard error of four experiments for each set. The *lines* represent the best fit of a simple rectangular hyperbola, sharing the top for all curves and the bottom at 0. The *dashed lines* simply connect the data points when no inhibition was measured. **Top Panel.** Inhibition of signaling by Compound **2**. The top of the shared curve-fit was estimated at $105 \pm 2.7\%$, constraining the slope factor at 1. Estimates of pIC_{50} for Compound **2** were 7.6 ± 0.11 (CCR4 WT), 5.5 ± 0.11 (CCR4-5T), 6.1 ± 0.91 (CCR5 WT) and 7.5 ± 0.85 (CCR5-4T). **Middle Panel.** Inhibition of signaling by the CCR4 antagonist BMS-397. Fitted curves were constrained with a slope factor of 1 and the top of the curve at 100. Estimates of pIC_{50} for BMS-397 were 7.29 ± 0.40 (CCR4 WT) and 6.91 ± 0.038 (CCR4-5T). SCH-C was inactive at both CCR4 WT and CCR4-5T. **Bottom Panel.** Inhibition of signaling by the CCR5 antagonist SCH-C. Fitted curves were constrained with the top of the curve at 100. Estimates of pIC_{50} for SCH-C were 7.58 ± 0.062 (CCR5 WT) and 8.18 ± 0.063 (CCR5-4T), with the shared slope factor estimated at 1.4 ± 0.19 for both curves. BMS-397 was inactive at both CCR5 WT and CCR5-4T.

MOL 39321

Table 1

Effect of cell permeabilization to normalize binding potencies in cells and membranes for selected pyrazinyl-sulfonamides at CCR4

Compound	pIC ₅₀			
	CHO Membrane	CHO Cell	Membrane + saponin	Cell + saponin
5	6.7 ± 0.35 (3)	6.7 ± 0.47 (3)	6.6 ± 0.49 (3)	6.7 ± 0.50 (3)
9	7.2 ± 0.10 (4)	8.3 ± 0.25 (4)	7.2 ± 0.12 (4)	7.2 ± 0.25 (4)
10	7.8 ± 0.27 (5)	8.3 ± 0.23 (5)	7.8 ± 0.36 (3)	7.9 ± 0.20 (3)
Carboxylic acid derivative of 9	7.5 ± 0.14 (4)	5.7 ± 0.25 (3)	7.9 ± 0.17 (4)	7.8 ± 0.18 (4)

Competition for the specific binding of 1 nM [³H]Cmpd-1 was measured for the CCR4 antagonists following equilibration with CCR4 in CHO membranes or cells in the presence or absence of saponin as described in Materials and Methods. Fitted estimates of pIC₅₀ from separate experiments were calculated and the average and standard deviation are shown (the value in parentheses represents the number of experiments).

MOL 39321

Table 2

Dependency on host cell for binding potencies of selected pyrazinyl-sulfonamides at recombinant CCR4

Compound	pIC ₅₀		
	CHO Membrane	CHO Cell	HEK Cell
2	8.0 ± 0.40 (7)	7.6 ± 0.10 (6)	7.7 ± 0.20 (7)
6	7.4 ± 0.15 (4)	5.4 ± 0.10 (4)	6.4 ± 0.12 (7)
8	7.6 ± 0.19 (8)	6.5 ± 0.22 (5)	7.5 ± 0.19 (5)

Competition for the specific binding of 1 nM [³H]Cmpd-1 was measured for the CCR4 antagonists following equilibration with CCR4 in CHO membranes or HEK-Gq_{i5} cells as described in Materials and Methods. Inhibition of the specific binding of FB-CCL22 was measured for the same CCR4 antagonists following equilibration with CCR4-CHO cells, also described in Materials and Methods. Fitted estimates of the pIC₅₀ were measured in separate experiments and the average and standard error were calculated and shown above (the value in parentheses represents the number of experiments)

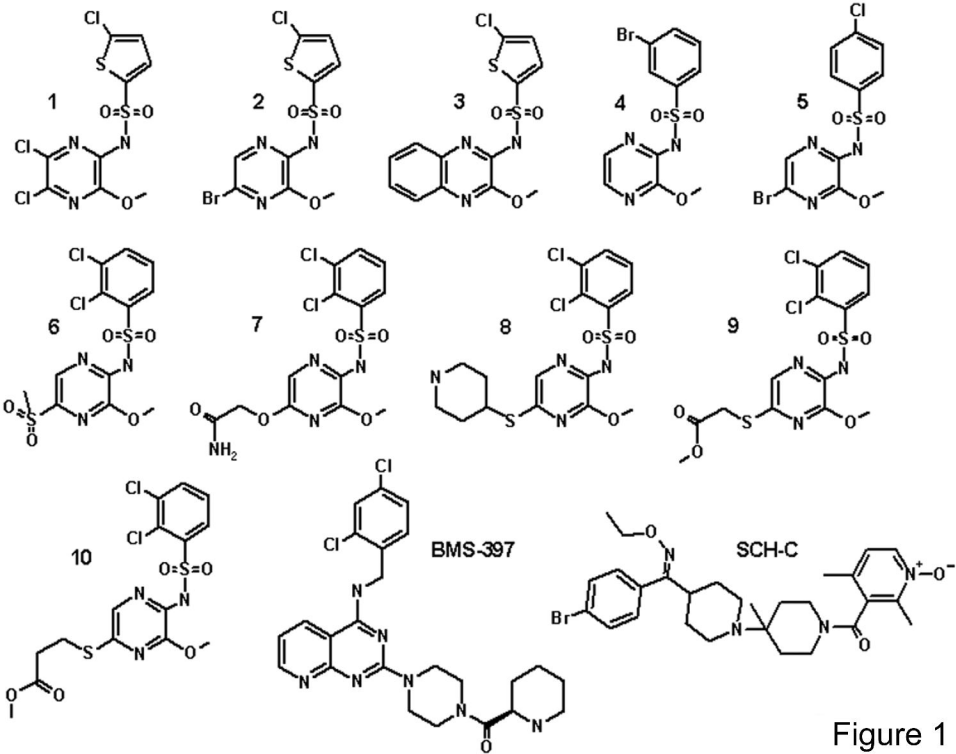


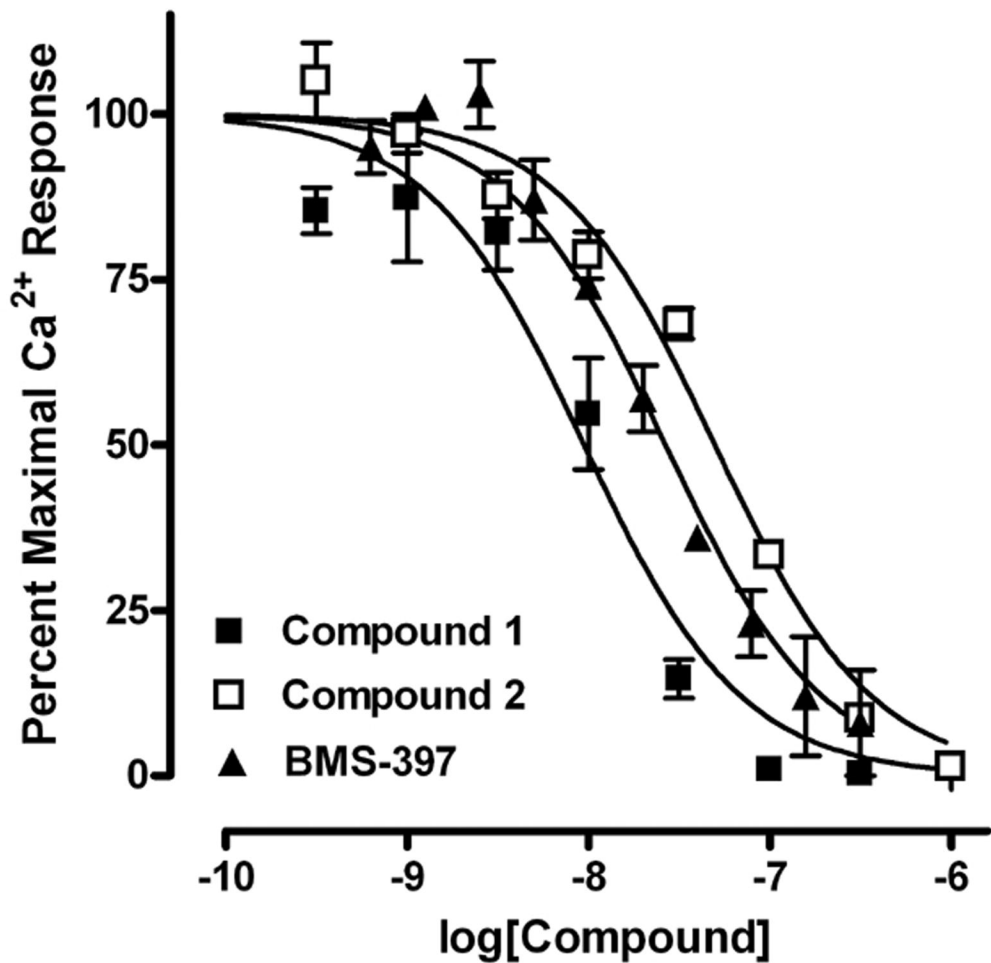
Figure 1

CCR4:	vElevLqdCt	fer yLDyAi Q	aTETLafv	HC	CINPIIY	FF	l	GEKFRkYiLq
CCR5:	qEfgLnnCs	ssnrLDqAmQ	vTETLgmt	HC	CiNP I I Y	aFv		GEKFRnYlLv
Consensus:	-E---L--C-	----LD-A-Q	-TETL---	HC	C-NP I I Y	F-		GEKFR-Y-L-

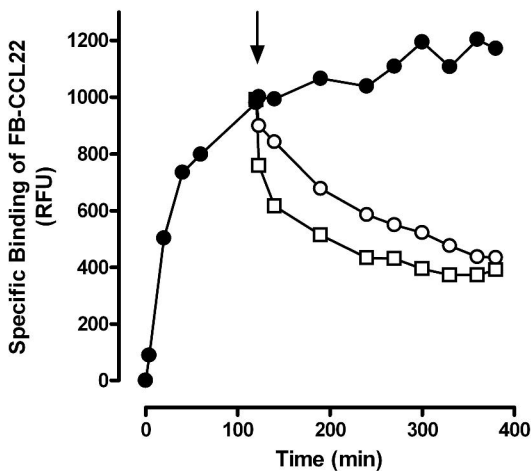
CCR4:	lF.KtcrglF	vICqyCgllQ	iysadtpSSs	YTqSTmdhdl	hdaL
CCR5:	fFqKhiakrF	. . CkcCsifQ	qeaperassv	YTrSTgeqei	svgl
Consensus:	-F-K-----F	--C--C---Q	-----SS-	YT-ST-----	---L

Figure 2

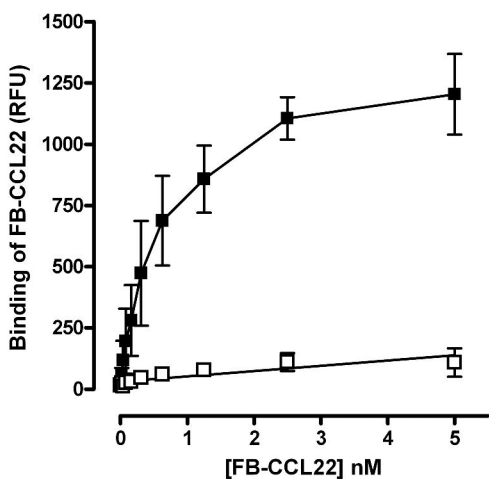
Figure 3



A



B



C

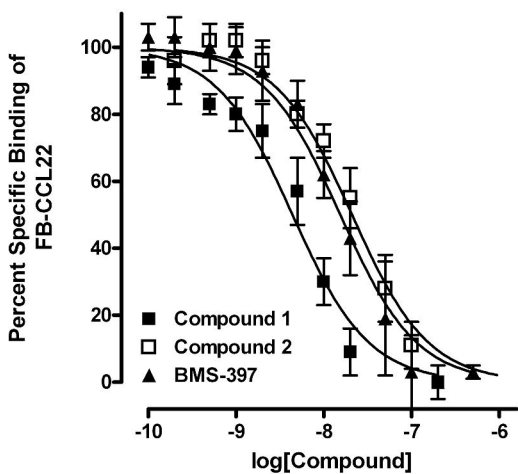


Figure 5

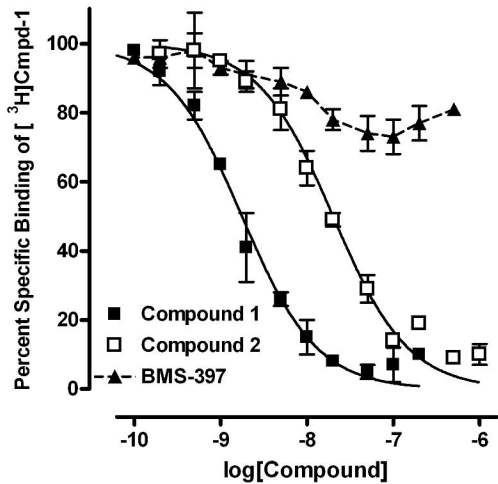
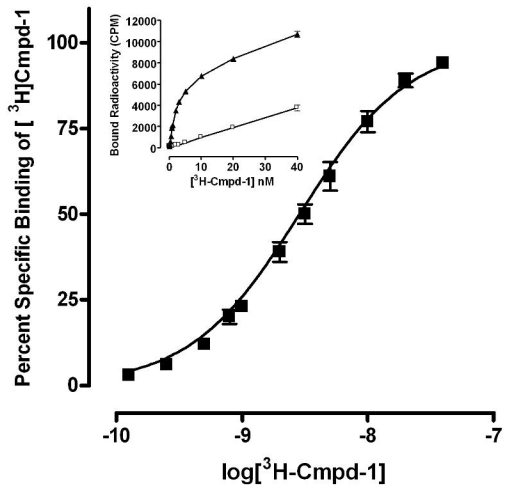
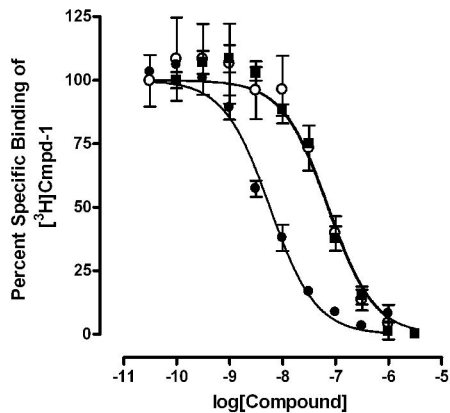
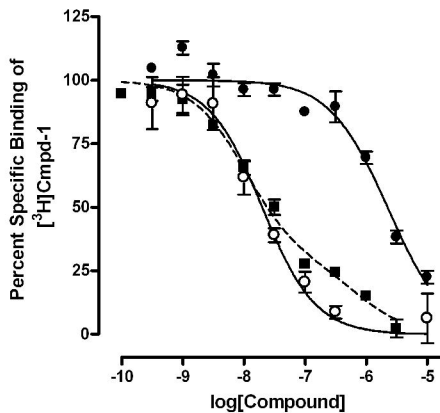
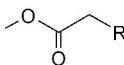
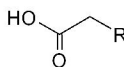
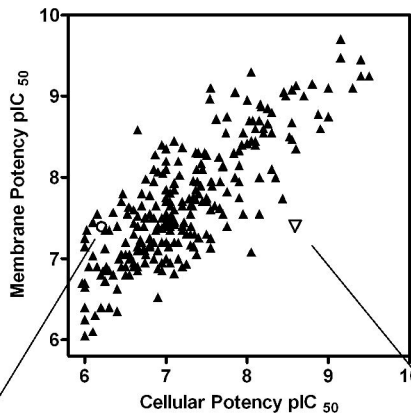
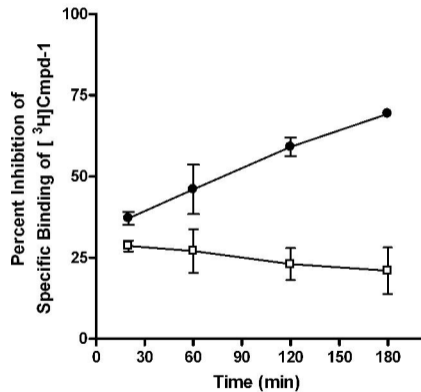


Figure 6



A



B

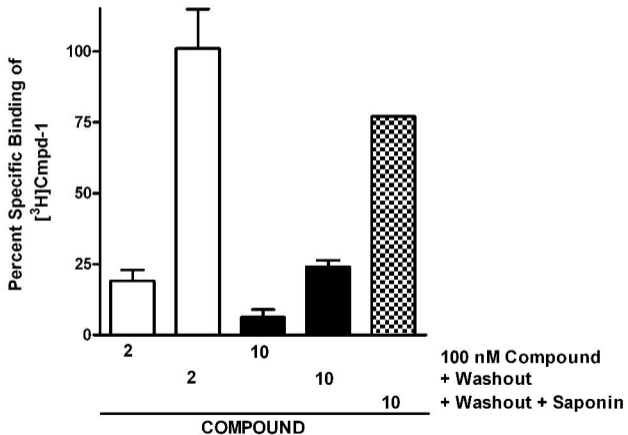
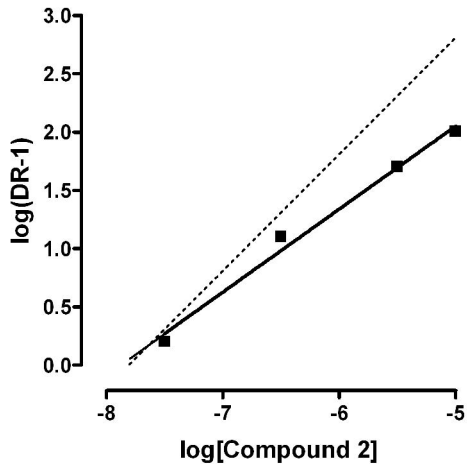
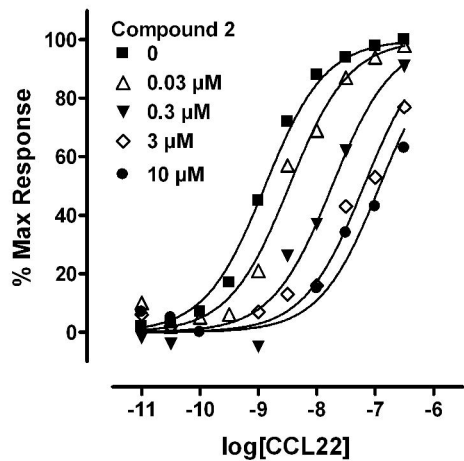
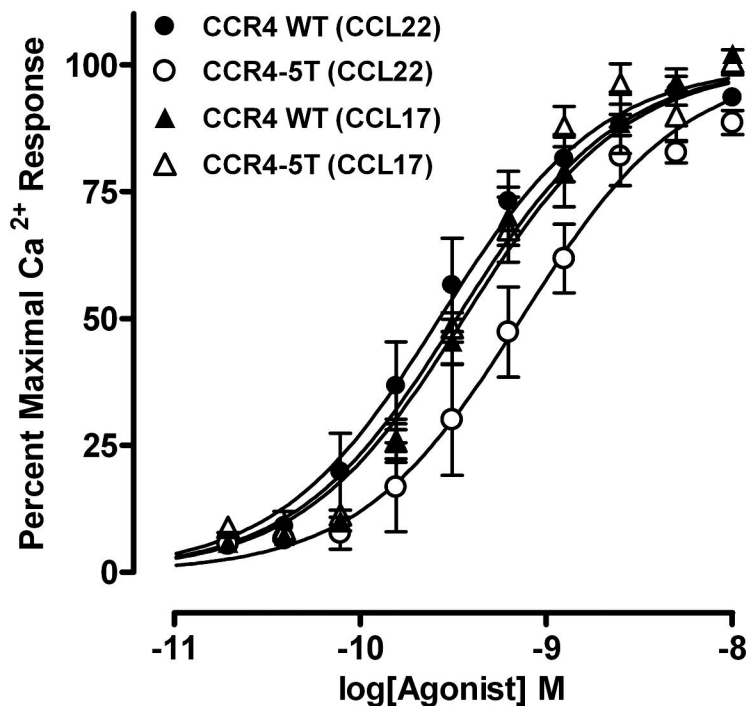


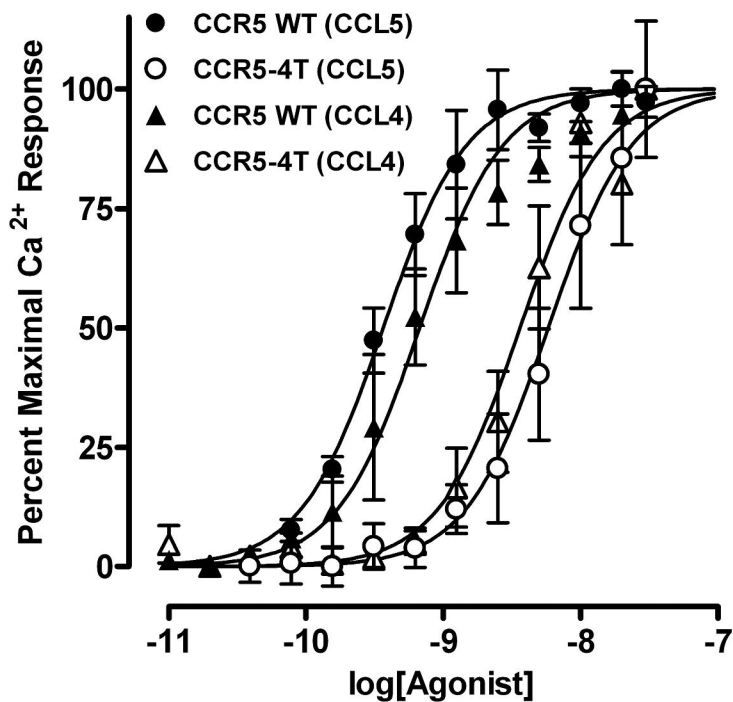
Figure 8



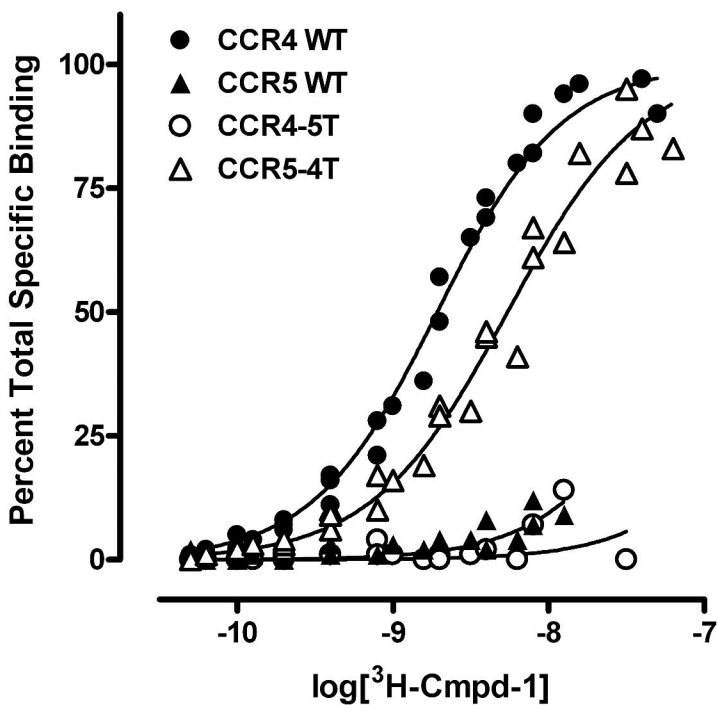
A



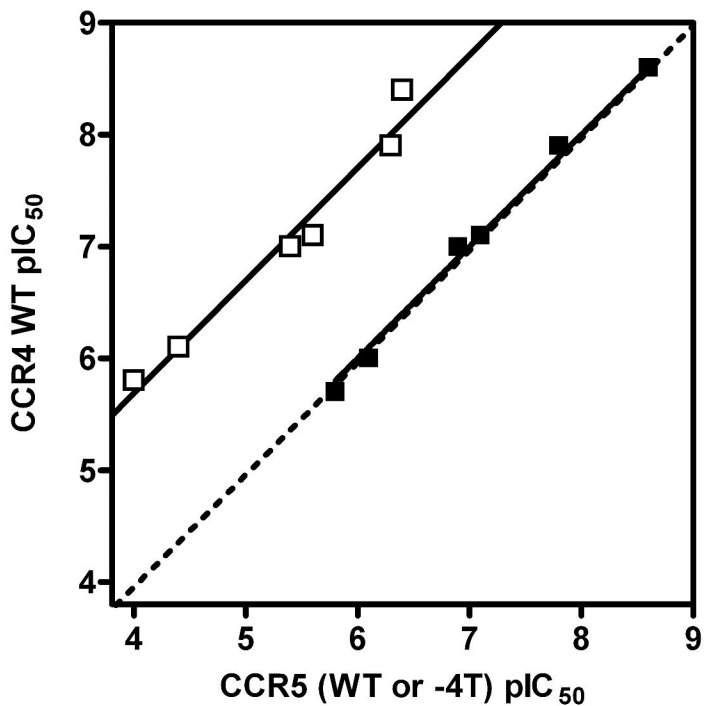
B

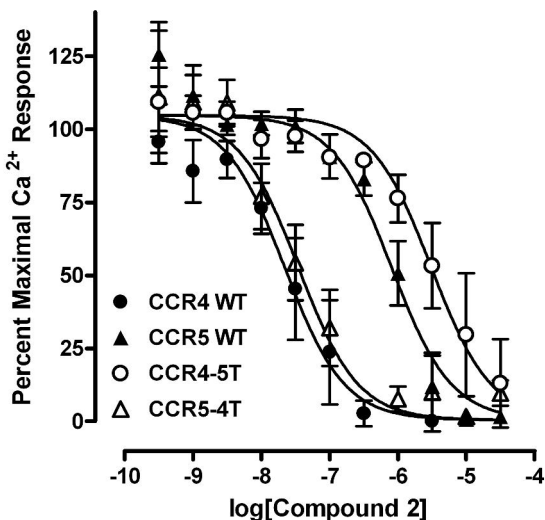


A



B



A**B**